

Evidence for a missing nucleon resonance in kaon photoproduction

T. Mart

Jurusan Fisika, FMIPA, Universitas Indonesia, Depok 16424, Indonesia

C. Bennhold

*Center for Nuclear Studies, Department of Physics, The George Washington University,
Washington, D.C. 20052, USA*

(September 6, 2018)

Abstract

New SAPHIR $p(\gamma, K^+)\Lambda$ total cross section data show a resonance structure at a total c.m. energy around 1900 MeV. We investigate this feature with an isobar model and find that the structure can be well explained by including a new D_{13} resonance at 1895 MeV. Such a state has been predicted by a relativistic quark model at 1960 MeV with significant γN and $K\Lambda$ branching ratios. We demonstrate how the measurement of the photon asymmetry can be used to further study this resonance. In addition, verification of the predicted large decay widths into the ηN and $\eta' N$ channels would allow distinguishing between other nearby D_{13} states.

PACS number(s): 14.20.Gk, 25.20.Lj, 13.60.Le, 13.30.Eg

The physics of nucleon resonance excitation continues to provide a major challenge to hadronic physics [1] due to the nonperturbative nature of QCD at these energies. While methods like Chiral Perturbation Theory are not amenable to N^* physics, lattice QCD has only recently begun to contribute to this field. In a recent study [2] the excitation energies of $1/2^-$ and $3/2^-$ baryon resonances are calculated for the first time on the lattice with improved actions. The results show a clear splitting of these states from the ground state nucleon, demonstrating the potential and the promise of extracting N^* structure from lattice QCD. However, most of the theoretical work on the nucleon excitation spectrum has been performed in the realm of quark models. Models that contain three constituent valence quarks predict a much richer resonance spectrum [3,4] than has been observed in $\pi N \rightarrow \pi N$ scattering experiments. Quark model studies have suggested that those "missing" resonances may couple strongly to other channels, such as the $K\Lambda$ and $K\Sigma$ channels [5] or final states involving vector mesons.

The newly established electron and photon facilities have made it possible to investigate the mechanism of nucleon resonance excitation with photons with much improved experimental accuracy. Experiments with kaon-hyperon final states have been performed at ELSA [6] and are being analyzed at JLab. Much improved data are becoming available in the $p(\gamma, K^+)\Lambda$, $p(\gamma, K^+)\Sigma^0$ and $p(\gamma, K^0)\Sigma^+$ channels, from total cross section to polarization observables. The new SAPHIR total cross section data [6] for the $p(\gamma, K^+)\Lambda$ channel, shown in Fig. 1, indicate for the first time a structure around $W = 1900$ MeV. This structure could not be resolved before, due to the low quality of the old data. It is the purpose of this paper to investigate this structure in the framework of an isobar model.

Pioneered by Thom [7], most studies over the last 30 years analyzed the $N(\gamma, K)\Lambda(\Sigma)$ in a tree-level isobar framework [8–11] that included a number of resonances whose couplings were adjusted to reproduce the experimental data. Due to the poor data quality it was not possible to decide which resonances contributed, even the magnitude of the background terms was uncertain. Recently, two new developments have provided significant progress in this field. First, a coupled-channels calculation that included final-state interactions [12] linked the photoproduction process $p(\gamma, K^+)\Lambda$ to the hadronic process $p(\pi^-, K^0)\Lambda$. Secondly, the recent work on including hadronic form factors in photoproduction reactions [13,14] while maintaining gauge invariance has resulted in the proper description of the background terms, allowing the use of approximate SU(3) symmetry to fix the Born coupling constants $g_{K\Lambda N}$ and $g_{K\Sigma N}$.

Due to their isospin structure the $K\Sigma$ photoproduction channels can involve the excitation of N^* as well as Δ states. On the other hand, $K\Lambda$ photoproduction only involves intermediate isospin $1/2$ resonances and is therefore easier to describe. Here, we use the tree-level isobar model described in Ref. [15] to analyze the $p(\gamma, K^+)\Lambda$ process in more detail. Guided by a recent coupled-channels analysis [12], the low-energy resonance part of this model includes three states that have been found to have significant decay widths into the $K^+\Lambda$ channel, the $S_{11}(1650)$, $P_{11}(1710)$, and $P_{13}(1720)$ resonances. In order to approximately account for unitarity corrections at tree-level we include energy-dependent widths along with partial branching fractions in the resonance propagators [15]. The background part includes the standard Born terms along with the $K^*(892)$ and $K_1(1270)$ vector meson poles in the t -channel. As in Ref. [15], we employ the gauge method of Haberzettl [13,14] to include hadronic form factors. The fit to the data was significantly improved by allowing for

separate cut-offs for the background and resonant sector. For the former, the fits produce a soft value around 800 MeV, leading to a strong suppression of the background terms while the resonant cut-off is determined to be 1900 MeV.

As shown in Fig. 1, our model cannot reproduce the SAPHIR total cross section data without inclusion of a new resonance with a mass of around 1900 MeV. While there are no 3- or 4-star isospin 1/2 resonances around 1900 MeV in the Particle Data Table [16], several 2-star states are listed. Of those only the $D_{13}(2080)$ state has been identified in older $p(\pi^-, K^0)\Lambda$ analyses [17,18] to have a noticeable branching ratio into the $K\Lambda$ channel. On the theoretical side, the constituent quark model by Capstick and Roberts [4] predicts many new states around 1900 MeV; however, only a few of them have been calculated to have a significant $K\Lambda$ decay width [5]. These are the $[S_{11}]_3(1945)$, $[P_{11}]_5(1975)$, $[P_{13}]_4(1950)$, and $[D_{13}]_3(1960)$ states, where the subscript refers to the particular band that the state is predicted in. We have performed fits for each of these possible states, allowing the fit to determine the mass, width and coupling constants of the resonance. We found that all four states can reproduce the structure at W around 1900 MeV, reducing the χ^2/N from around 4.5 to around 3 in each case. Table I compares our extracted resonance parameters with the quark model predictions of Ref. [5]. While all four of the above resonances have large decay widths into the $K\Lambda$ channel, only the $D_{13}(1960)$ state is predicted to also have significant photocouplings. Table I presents the remarkable agreement, up to the sign, between the quark model prediction and our extracted results for the $D_{13}(1960)$. The sign remains ambiguous, since at this stage we only extract the product of coupling constants. For the other three states the partial widths extracted from our fit overestimate the quark model results by up to a factor of 30.

How reliable are the quark model predictions? Clearly, one test is to confront its predictions with the extracted couplings for the well-established resonances in the low-energy regime of the $p(\gamma, K^+)\Lambda$ reaction, the $S_{11}(1650)$, $P_{11}(1710)$ and $P_{13}(1720)$ excitations. Table II shows that the magnitudes of the extracted partial widths for the $S_{11}(1650)$, $P_{11}(1710)$, and $P_{13}(1720)$ are in good agreement with the quark model. Therefore, even though the remarkable quantitative agreement in the case of the $D_{13}(1960)$ is probably fortuitous, we believe the structure in the SAPHIR data is in all likelihood produced by this particular resonance. Is this state identical to the 2-star resonance $D_{13}(2080)$ listed in the Particle Data Table? Table III displays a list of D_{13} states below 2.2 GeV predicted by Refs. [4,5], along with the Particle Data Table listings. A closer examination of the literature reveals that there is some evidence for two resonances in this wave between 1800 and 2200 MeV [19]; one with a mass centered around 1900 MeV and another with mass around 2080 MeV. It is the former which has been seen prominently in two separate $p(\pi^-, K^0)\Lambda$ analyses [17,18]. Thus, we believe that the state appearing in the SAPHIR data is in fact identical to the one seen in hadronic $K\Lambda$ production and corresponds to the $D_{13}(1960)$ state predicted by the quark model. The D_{13} excitation around 2080 MeV seen in Refs. [19,20] may well correspond to the quark model state $D_{13}(2055)$ in the $N = 4$ band. In order to clearly separate these nearby D_{13} states, measuring other channels will be helpful. For example, Ref. [4] predicts the $D_{13}(1960)$ to have large decay widths into the ηN and $\eta' N$ channels, in contrast to the $D_{13}(2055)$ whose branching ratios into these channels are negligible.

Figure 1 compares our models with and without the $D_{13}(1960)$ with the SAPHIR total cross section data. Our result without this resonance shows only one peak near threshold,

while inclusion of the new resonance leads to a second peak at W slightly below 1900 MeV, in accordance with the new SAPHIR data. The difference between the two calculations is much smaller for the differential cross sections, as displayed in Fig. 2. As expected, including the $D_{13}(1960)$ does not affect the threshold and low-energy regime while it does improve the agreement at higher energies. Figure 3 compares the recoil polarization for the two calculations. Clearly, the differences are small for all angles, demonstrating that the recoil polarization is not the appropriate observable to further study this resonance.

The target asymmetry of $K^+\Lambda$ photoproduction is shown in Fig. 4. Here we find larger variations between the two calculations, especially for higher energies. The three data points seem to favor a model without the new $D_{13}(1960)$; however, more complete and accurate measurements are clearly needed over the whole angular range before any conclusion can be drawn. The largest effects are found in the photon asymmetry shown in Fig. 5. For $W \geq 1800$ MeV, including the new resonance leads to a sign change in the photon asymmetry whose magnitude is almost one at intermediate angles. Therefore, we would suggest that measuring this observable is well suited to shed more light on the contribution of this state in kaon photoproduction.

In conclusion, we have investigated the structure around $W = 1900$ MeV in the new SAPHIR total cross section data in the framework of an isobar model. We found that the data can be well reproduced by including a new D_{13} resonance with a mass, width and coupling parameters in good agreement with the values predicted by a recent quark model calculation. To further elucidate the role and nature of this state we suggest measurements of the polarized photon asymmetry around $W = 1900$ MeV for the $p(\gamma, K^+)\Lambda$ reaction. With the arrival of new, high-precision cross section and polarization data the kaon photoproduction process will be able to unfold its full potential in the search and study of nucleon resonances.

TM thanks the member of the Center for Nuclear Studies for the hospitality extended to him during his stay in Washington, D.C. This work was supported by the University Research for Graduate Education (URGE) grant (TM), and US DOE grant DE-FG02-95ER-40907 (CB).

REFERENCES

- [1] *Proceedings of the 4th Workshop on N^* Physics*, Washington, D.C., 1997, edited by H. Haberzettl, C. Bennhold, and W. J. Briscoe, πN Newsletter **14**, 1 (1998).
- [2] F. X. Lee and D. B. Leinweber, 'Negative-parity Baryon Spectroscopy', hep-lat/9809095 (1998).
- [3] N. Isgur and G. Karl, Phys. Lett. B **72**, 109 (1977); Phys. Rev. D **23**, 817 (1981); R. Koniuk and N. Isgur, Phys. Rev. D **21**, 1868 (1980).
- [4] S. Capstick and W. Roberts, Phys. Rev. D **49**, 4570 (1994).
- [5] S. Capstick and W. Roberts, Phys. Rev. D **58**, 074011 (1998).
- [6] SAPHIR Collaboration: M. Q. Tran *et al.*, Phys. Lett. B **445**, 20 (1998).
- [7] H. Thom, Phys. Rev. **151**, 1322 (1966).
- [8] R. A. Adelseck, C. Bennhold, and L. E. Wright, Phys. Rev. C **32**, 1681 (1985).
- [9] R. A. Williams, C.-R. Ji, and S. R. Cotanch, Phys. Rev. C **46**, 1617 (1992).
- [10] T. Mart, C. Bennhold, and C. E. Hyde-Wright, Phys. Rev. C **51**, R1074 (1995).
- [11] J. C. David, C. Fayard, G. H. Lamot, and B. Saghai, Phys. Rev. C **53**, 2613 (1996).
- [12] T. Feuster and U. Mosel, Phys. Rev. C **58**, 457 (1998); Phys. Rev. C **59**, 460 (1999).
- [13] H. Haberzettl, Phys. Rev. C **56**, 2041 (1997).
- [14] H. Haberzettl, C. Bennhold, T. Mart, and T. Feuster, Phys. Rev. C **58**, R40 (1998).
- [15] C. Bennhold, T. Mart, A. Waluyo, H. Haberzettl, G. Penner, T. Feuster, and U. Mosel, in *Proceedings of the Workshop on Electron Nucleus Scattering*, Elba, Italy, 1998 (in press), nucl-th/9901066 (1999); H. Haberzettl, C. Bennhold, T. Mart, and T. Feuster, in *Proceedings of Baryons '98*, Bonn, Germany, 1998 (in press), nucl-th/9811024 (1998); Few-Body Syst. Suppl. **10**, 515 (1999).
- [16] C. Caso *et al.*, Eur. Phys. J. C **3**, 1 (1998).
- [17] D. H. Saxon *et al.*, Nucl. Phys. **B162**, 522 (1980).
- [18] K. W. Bell *et al.*, Nucl. Phys. **B222**, 389 (1983).
- [19] R. E. Cutkosky, C. P. Forsyth, J. B. Babcock, R. L. Kelly, and R. E. Hendrick, in *Proceedings of the 4th Int. Conference on Baryon Resonances, Baryon 1980*, Toronto, Canada, 1980, edited by N. Isgur, p. 19; R. E. Cutkosky, C. P. Forsyth, R. E. Hendrick, and R. L. Kelly, Phys. Rev. D **20**, 2839 (1979).
- [20] G. Höhler, F. Kaiser, R. Koch, E. Pietarinen, Physics Data, No. 12-1 (1979); in *Proceedings of the 4th Int. Conference on Baryon Resonances, Baryon 1980*, Toronto, Canada, 1980, edited by N. Isgur, p. 3.
- [21] S. Capstick, Phys. Rev. D **46**, 2864 (1992).
- [22] Aachen-Berlin-Bonn-Hamburg-Heidelberg-München Collaboration, Phys. Rev. **188**, 2060 (1969). A list of references for the old data can be found in Ref. [6].

TABLES

TABLE I. Comparison between the results from our fit to the kaon photoproduction data $p(\gamma, K^+)\Lambda$ (Fit) and those of the quark model (QM), where the QM photocouplings were taken from Ref. [21] and the $K\Lambda$ decay widths from Ref. [5].

Missing Resonance	Model	m_{N^*} (MeV)	Γ_{N^*} (MeV)	$\sqrt{\Gamma_{N^*N\gamma}\Gamma_{N^*K\Lambda}}/\Gamma_{N^*}$ (10^{-3})
$S_{11}(1945)$	Fit	1847	258	-10.370 ± 0.875
	QM	1945	595	0.298 ± 0.349
$P_{11}(1975)$	Fit	1935	131	9.623 ± 0.789
	QM	1975	45	1.960 ± 0.535
$D_{13}(1960)$	Fit	1895	372	$2.292^{+0.722}_{-0.204}$
	QM	1960	535	-2.722 ± 0.729
$P_{13}(1950)$	Fit	1853	189	$1.097^{+0.011}_{-0.010}$
	QM	1950	140	-0.334 ± 0.070

TABLE II. Comparison between the extracted fractional decay widths and the result from the quark model [5,21] for the $S_{11}(1650)$, $P_{11}(1710)$, and $P_{13}(1720)$ resonances.

Resonance	$\sqrt{\Gamma_{N^*N\gamma}\Gamma_{N^*K\Lambda}}/\Gamma_{N^*}$ (10^{-3})	
	Extracted	Quark Model
$S_{11}(1650)$	-4.826 ± 0.051	-4.264 ± 0.984
$P_{11}(1710)$	1.029 ± 0.172	-0.535 ± 0.115
$P_{13}(1720)$	$1.165^{+0.041}_{-0.039}$	-1.291 ± 0.240

TABLE III. Summary of listed D_{13} resonances. The observed states from the Particle Data Table are ordered according to Refs. [4,5].

Quark Model [4,5]		Particle Data Table [16]	
Name		Name	Status
$[N\frac{3}{2}^-]_1(1495)$		$N(1520)D_{13}$	* * *
$[N\frac{3}{2}^-]_2(1625)$		$N(1700)D_{13}$	* * *
$[N\frac{3}{2}^-]_3(1960)$		$N(2080)D_{13}$	**
$[N\frac{3}{2}^-]_4(2055)$		-	-
$[N\frac{3}{2}^-]_5(2095)$		-	-
$[N\frac{3}{2}^-]_6(2165)$		-	-
$[N\frac{3}{2}^-]_7(2180)$		-	-

FIGURES

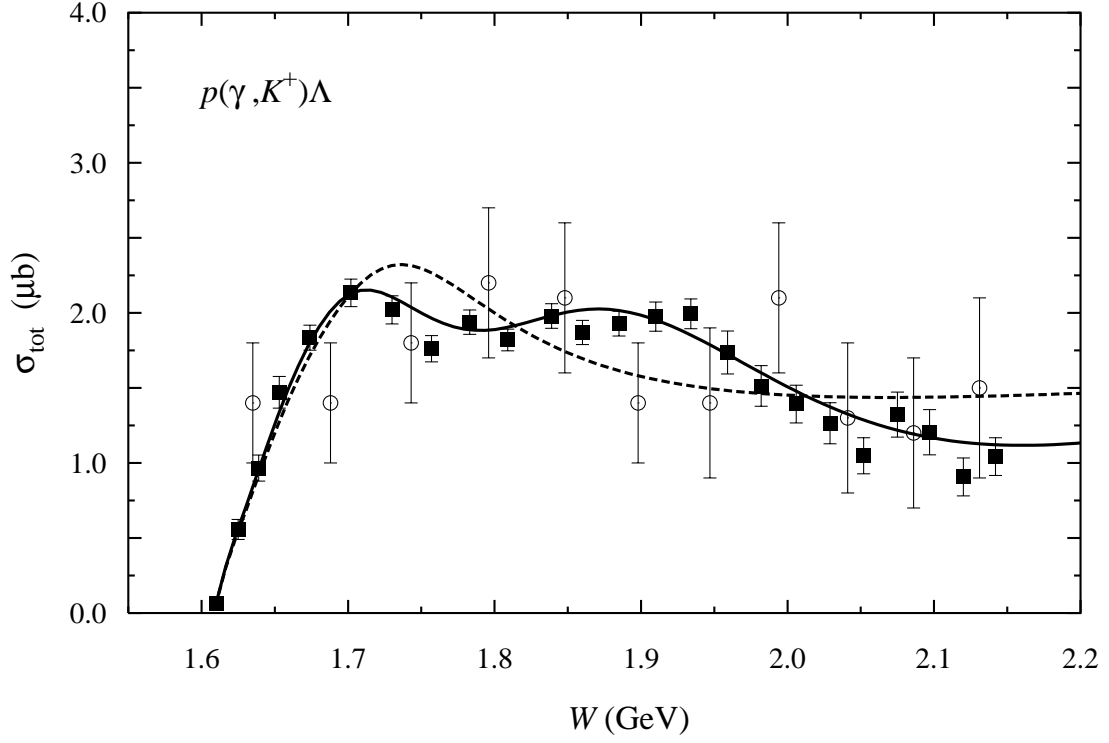


FIG. 1. Total cross section for $K^+\Lambda$ photoproduction on the proton. The dashed line shows the model without the $D_{13}(1960)$ resonance, while the solid line is obtained by including the $D_{13}(1960)$ state. The new SAPHIR data [6] are denoted by the solid squares, old data [22] are shown by the open circles.

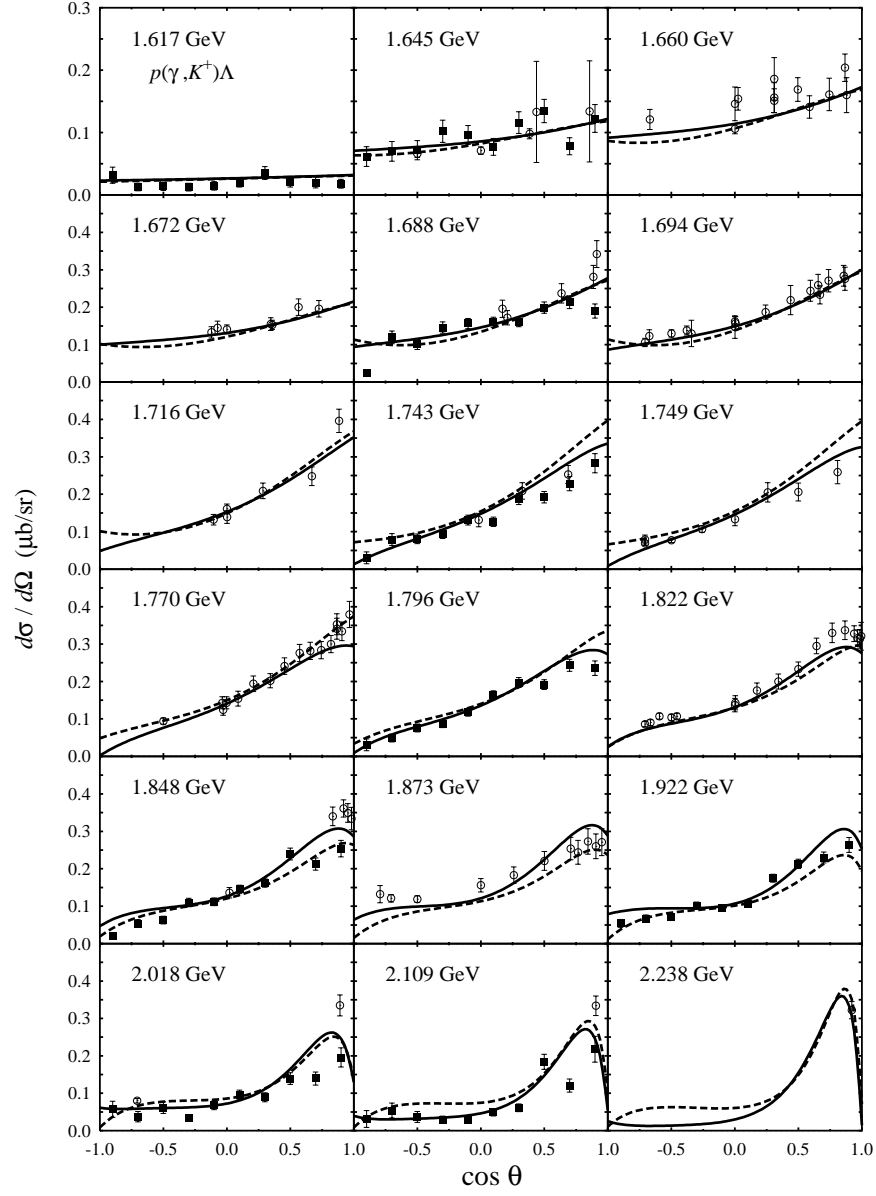


FIG. 2. Same as in Fig. 1 for the differential cross section. The total c.m. energy W is shown in every panel.

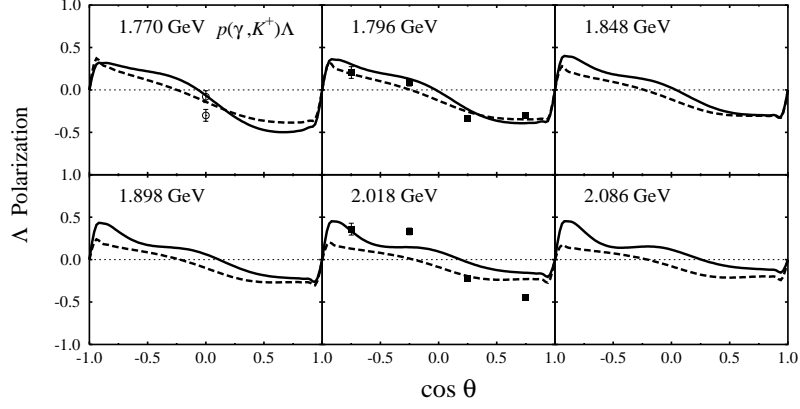


FIG. 3. Same as in Fig. 1 for the Λ recoil polarization. The total c.m. energy W is shown in every panel.

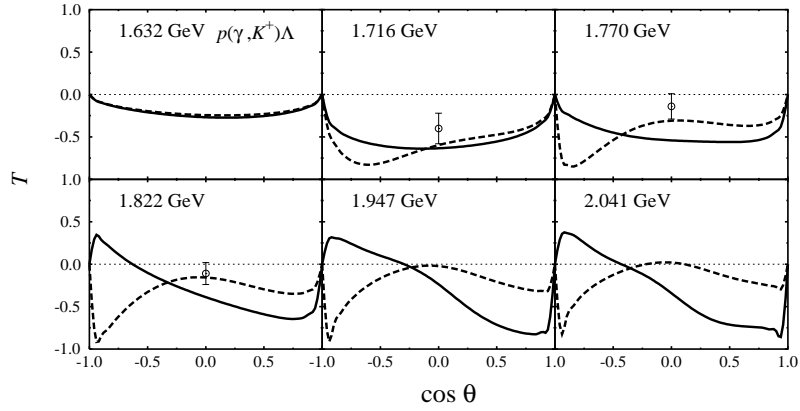


FIG. 4. Same as in Fig. 1 for the target polarization. The total c.m. energy W is shown in every panel.

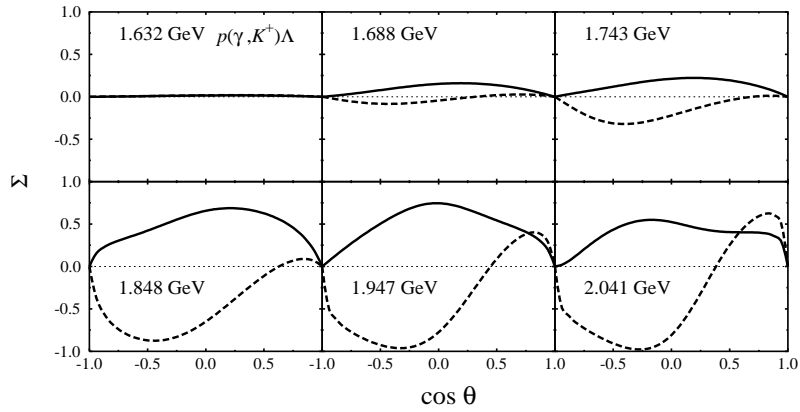


FIG. 5. Same as in Fig. 1 for the photon asymmetry. The total c.m. energy W is shown in every panel.